Understanding the Drivers of Land Surface Temperature Based on Multisource Data: A Spatial Econometric Perspective

Menghang Liu, Haitao Ma, and Yu Bai

***Abstract*—Urban thermal condition has seriously affected the quality of residents' daily life and triggered some environmental issues. Understanding spatial patterns of land surface temperature (LST) and its driving mechanism is important for the sustainable development of cities. Taking Beijing as an example, this study employed spatial econometric models to investigate spatial and temporal heterogeneity of LST from 2014 to 2018 based on multisource remote sensing and statistical data. The global autocorrelation Moran's I index showed the existence of significant positive correlations of LST among regions, indicating the regions with high thermal environments are spatially adjacent. The temperature of a region would increase by more than 0.6% for every 1% increase in LST of surrounding areas based on the spatial Durbin model. In terms of spatial interactions of influencing factors, elevation, normalized difference vegetation index, modified normalized difference water index, nighttime light, and fossil energy consumption of neighbors exhibited significantly positive spatial agglomeration effects on local LST, whereas albedo, GDP, and population density of adjacent areas had negative effects on LST in local areas. Particularly, the indirect effects of drivers were greater than their direct effects, indicating urban thermal condition was an interregional issue and joint control measures should be adopted to mitigate the urban heat island effects as a whole.**

***Index Terms*—Beijing, direct and indirect effects, land surface temperature (LST), spatial durbin model (SDM).**

I. Introduction

IN RECENT decades, China has experienced the expansion of urban scale and population, and it is currently in the stage of rapid urbanization [1], [2]. According to the report published by United Nations in 2018, more than 55% of the world's population live in urban areas, and this proportion is expected to increase to 68% by 2050 [3]. High population agglomeration and rapid urban spread have remarkably accelerated the alteration of the land surface. Natural features such as vegetation and water bodies have been replaced by impervious materials and buildings. These impervious surfaces with high thermal capacity led to a significant changing trend in land surface temperature (LST), which has altered the original urban energy balance [4]–[7]. This transition poses a threat to social and environmental issues, such as human health [8], energy consumption [9], heat waves [10], air pollution [11], and climate change [12]–[14]. Therefore, a deep investigating of the spatial patterns of LST is critically significant to support eco-friendly and sustainable urban planning.

LST is a result of the interaction of multiple influencing factors, thus understanding the driving mechanisms of these factors is a prerequisite for targeted mitigation. Numerous studies have concluded that LST is distinct significantly from various land use types [15], [16]. Impervious surfaces, such as residential and industrial land use, modify the urban microclimate in built-up areas, whereas vegetation, water bodies, and wetland parks can be regarded as "cold islands" to mitigate the local heat island effects. The transformation of land cover alters water infiltration and thermal conductivity. Consequently, landscape pattern metrics have been widely used to measure the relationships between land use type and LST [17]–[20]. Some surface biophysical parameters based on remote sensing, such as normalized difference vegetation index (NDVI) and modified normalized difference water index (MNDWI), are successfully applied to qualitatively describe land cover characteristics, due to its effectiveness to acquire broad scale and long time series data on the Earth's surface. The easy access, wide coverage, and high resolution of remote sensing pave the way for urban thermal environmental research. Meanwhile, socio-economic indicators are been considered as a complement of remote sensing data in terms of investigating driving factors on LST [21]–[24]. The agglomerations of population and economic activities trigger urban thermal environments. Human activities consume large quantities of fossil fuel resources for urban construction, and anthropogenic heat emissions further increase the thermodynamic properties of the land surface. Besides, the land surface has a greater tendency to absorb solar radiation by contrast with water bodies, and has a lower albedo [25]. Differences in topography, such as slope and elevation, also play an important

Manuscript received October 1, 2021; revised November 9, 2021; accepted November 19, 2021. Date of publication November 23, 2021; date of current version December 10, 2021. This work was supported in part by the Second Tibetan Plateau Scientific Expedition and Research Program under Grant 2019QZKK1005, in part by the National Natural Science Foundation of China under Grant 41590842, and in part by the National Key Research and Development Program of China under Grant 2016YFC0503006. *(Corresponding author: Haitao Ma.)*

Menghang Liu and Haitao Ma are with the Key Laboratory of Regional Sustainable Development Modeling, Institute of Geographic Sciences and Natural Resources Research, Chinese Academy of Sciences, Beijing 100101, China (e-mail: liumh25@163.com; maht@igsnrr.ac.cn).

Yu Bai is with the Laboratory of Ecosystem Network Observation and Modeling, Institute of Geographic Sciences and Natural Resources Research, Chinese Academy of Sciences, Beijing 100101, China, and also with the University of Chinese Academy of Sciences, Beijing 100049, China (e-mail: yubaimail@163.com).

Digital Object Identifier 10.1109/JSTARS.2021.3129842

role in controlling the amount of radiation absorbed by the surface [26], and would fundamentally alter the land surface thermal condition. It is crucial to conduct a comprehensive analysis of multisource data to explore interaction mechanisms of LST.

In order to explore the nexus between LST and its drivers, ordinary least-squares (OLS) regression has typically been used [27], [28]. However, traditional regression analysis based on the independent assumption of variables may neglect the spatial heterogeneity and spillover effects of LST, thus, substantially hindering insight into the interpretation of urban thermal condition. The thermodynamic properties of the land surface have significant spatial aggregation and diffusion effects because of heat conduction and cross-ventilation. That is, it presents strong spatial autocorrelation among thermal intensity and distribution. Moreover, an increasing number of literatures use cross-sectional data, which are more likely to cause multicollinearity problems and reduce the accuracy of results [29]. Spatial econometric models, specifically the spatial panel data model, are effective for identifying the impact of determinants on LST, which can capture the impact of adjacent areas on urban thermal environments and reflect interregional spatial heterogeneity.

A large body of studies have adopted a gridded unit to conduct research [30]–[33], mainly because the LST data derived from remote sensing is raster imagery. However, the application of raster-based data could come across problems during choosing the appropriate spatial resolutions. Some scholars analyzed spatial-temporal characteristics of LST from the perspective of landscape patches [34], [35], which may hinder the implementation of mitigation strategies in administrative districts. In China, regulatory planning has been considered as an indispensable complement of urban planning [8]. The district unit, regarding as the basic regulatory unit of shaping urban morphology, plays a significant role in land use planning and public infrastructure construction. Previous studies mainly used local climate zones [36], urban function zones [37], and urban green space [38] as the study units for analysis, and explored the heterogeneity of LST in different classified zones. These special units may concern land use configuration of the urban area, but ignore the implementation of mitigation strategies because regulatory planning is formulated at the administrative level. With this regard, we employ the averaged LST within the district unit to analyze urban thermal environments at the district level [39], which facilitates the plan formulation. And the driving factors can also be enriched by the data of the local statistics department.

In this article, we investigate the spatiotemporal patterns of LST and its related factors in Beijing at the district level via multi-source remote sensing and statistical data. There are three main contributions of this research as follows.

1) Considering the complexity and comprehensiveness of LST, we observed the impacts of multisource data, namely, solar radiation, topographical features, surface biophysical parameters, and socio-economic indicators, on local thermal environments.
2) We incorporated the spatial spillover effects into the empirical study, which has supplemented the spatial features of LST to a certain extent.

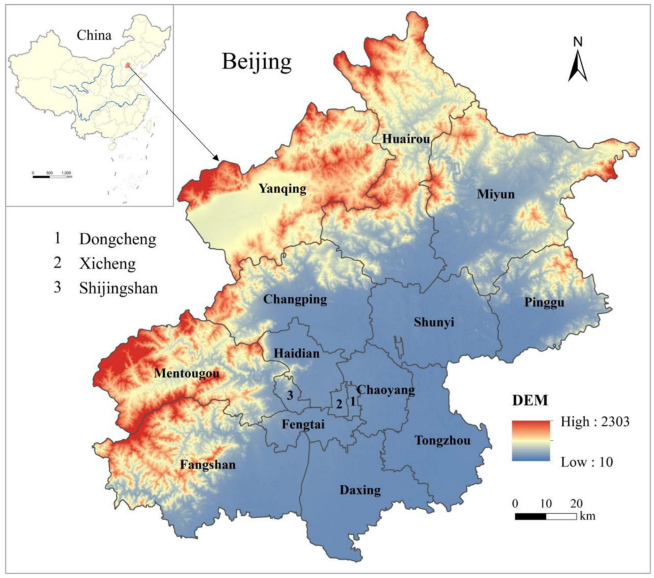

Fig. 1. Location of the study area.

3) We explored the distribution and determinants of LST focusing on the basic district level to strengthen the implementation of regional planning.

II. Study Area and Data

A. Study Area

Beijing (115°25′E-117°30′E, 39°28′N-41°05′N), the capital city of China, lies in north China plain and includes 16 administrative districts with the area of 16 410 km^2 (see Fig. 1). It has a temperate continental monsoon climate with humid-hot summer and dry-cold winter. The terrain is high in northwestern and low in southeast. Beijing has undergone rapid urbanization with the intensive expansion of built-up area and population in the 21st century, significantly altering urban climate characteristics. The increasing LST may further cause other urban issues and pose serious threats to residential comfort and sustainable urban development. Accordingly, it is of great importance to comprehensively investigate the spatiotemporal patterns and drivers of LST in Beijing.

B. Variables and Data Source

1) Dependent Variable: This article takes LST as the explained variable. LST data can be acquired through the retrieval of remote sensing images. Previous studies present that Moderate Resolution Imaging Spectroradiometer (MODIS) data have been widely used in LST inversion research [2], [40], [41]. The data used in the article was derived from 8-day MODIS daytime LST data (MOD11A2) products based on a split-window algorithm. We obtained LST data in Beijing from 2014 to 2018 at 1 km spatial resolution, provided by the National Aeronautics and Space Administration (NASA).[1]

2) Independent Variables: Based on the existing literature and data availability, this article selects ten variables under four

[1][Online]. Available: https://earthdata.nasa.gov

TABLE I
VARIABLES OF LST USED IN THIS ARTICLE

Dimension	Variable	Code	Reference	Source
Solar radiation	Albedo	ALB	[25, 44, 48]	GLASS
Topographical features	Slope	SLO	[26, 30, 49]	DEM
	Elevation	ELE	[14, 26, 48]	DEM
Surface biophysical parameters	Normalized difference vegetation index	NDVI	[5, 19, 50]	Landsat
	Modified normalized difference water index	MNDWI	[17, 20, 51]	Landsat
	Impervious area	IA	[21, 33, 52]	GAIA
Socio-economic indicators	Nighttime light	NTL	[13, 22, 53]	NPP-VIIRS
	Gross domestic product	GDP	[11, 23, 44]	Statistical Yearbook
	Population Density	PD	[4, 14, 23]	Statistical Yearbook
	Fossil Energy Consumption	FEC	[9, 32, 54]	Statistical Yearbook

dimensions as the explanatory variables to understand the spatial agglomeration effect of Beijing's LST at the district level (see Table I).

1) *Solar radiation*. The changes in land cover alter the heat absorption capacity of the surface. Buildings usually reduce the albedo and emissivity of surfaces, resulting in large surface heat storage in urban areas. Whereas vegetation with high albedos and high Bowen ratio may transmit little heat to the environment when exposed to solar radiation. Albedo data were obtained from Global Land Surface Satellite (GLASS) Albedo products, which are retrieved with direct-estimation methods and represent surface albedo under general clear-sky atmospheric conditions at 1 km spatial resolution [42]. The GLASS albedo, having been proved the superiority of capturing the variation of surface albedo than MODIS [43], [44], were downloaded from the National Earth System Science Data Sharing Infrastructure.[2]
2) *Topographical features*. The terrain affects the storage of surface heat, in turn changing the intensity of LST [14]. The ASTER Global Digital Elevation Model was employed in the study due to its high spatial resolution of 30 m, which was derived from the Geospatial Data Cloud of China.[3] After conducting the preprocess of projection transformation and surface analysis in ArcGIS 10.5, two topographical indicators, namely elevation and slope, were selected as independent variables.
3) *Surface biophysical parameters*. NDVI is a remote sensing indicator to distinguish vegetation and can be applied to detect vegetation changes and explain the impact of local thermal environments. MNDWI is used to extract water bodies. The loss of water and wetland through urban construction leads to an increased high thermal conductivity. NDVI and MNDWI were selected as driving factors to represent the urban surface characteristics, and these indicators were computed as follows:

$$\mathrm{NDVI} = \frac{\mathrm{NIR} - \mathrm{Red}}{\mathrm{NIR} + \mathrm{Red}} \tag{1}$$

$$\mathrm{MNDWI} = \frac{\mathrm{Green} - \mathrm{SWIR1}}{\mathrm{Green} + \mathrm{SWIR1}} \tag{2}$$

where NIR, Red, Green, and SWIR1 represent the near-infrared, red, green, and short-wave infrared-1 wave bands, respectively.

Landsat-8 datasets with sunny weather and low cloud cover were downloaded from the United States Geological Survey (USGS).[4] The datasets were first processed for radiometric calibration and atmospheric correction. Then NDVI and MNDWI were computed using the band math module in ENVI 5.3. Besides, the impervious surface area proportion can be considered as an important complement of remote sensing indicators in terms of capturing land cover features. It is calculated by dividing the impervious surface area by the total area of the local administrative unit. The impervious surfaces data were obtained from[5] and the details could be found by Gong *et al.* [45].

4) *Socio-economic indicators*. Nighttime light was widely used to assess economic development and anthropogenic activities, thus it is regarded as an important variable affecting LST [46]. The global VIIRS nighttime lights annual products were employed from an open access website[6] and detailed information such as data processing and accuracy evaluation could be found by Elvidge *et al.* [47]. The concentrations of economy and population in urban could lead to the increase of fossil energy consumption, thereby resulting in the higher temperature of the land surface. Therefore, gross domestic product, population density, and fossil energy consumption, derived from Beijing regional statistical yearbook,[7] are also selected to represent the impact of socio-economic activities on LST.

[2][Online]. Available: http://www.geodata.cn
[3][Online]. Available: http://www.gscloud.cn/
[4][Online]. Available: http://earthexplorer.usgs.gov
[5][Online]. Available: http://data.ess.tsinghua.edu.cn
[6][Online]. Available: https://eogdata.mines.edu/products/vnl
[7][Online]. Available: http://tjj.beijing.gov.cn

III. Methodology

A. Spatial Autocorrelation

The spatial dependence of a variable exhibits its spill-over effects between adjacent areas. The temperature of land surface may be agglomerated in areas with intensive economic activities, and regions close to it may have similar patterns. The most commonly adopted spatial autocorrelation indicator, global Moran's I, was selected to estimate the spatial relationship. It is calculated by the following formula:

$$I = \frac{n \cdot \sum_{i=1}^{n} \sum_{j=1}^{n} w_{ij} (x_i - \bar{x}) (x_j - \bar{x})}{\sum_{i=1}^{n} \sum_{j=1}^{n} w_{ij} \cdot \sum_{j=1}^{n} (x_i - \bar{x})^2} \tag{3}$$

where n denotes the total number of study units. W_{ij} is the spatial weight matrix, which uses geographic adjacency to set values. Generally, when i and j are adjacent, W_{ij} is indicated as 1, otherwise, the value is 0. x_i and x_j represent the LST of region i and j. $\bar{x}$ is the average value of LST among all regions. I represents global Moran's I index, the value of which ranges from -1 to 1. Normally, the larger the absolute value of the index, the stronger the spatial relationship. If the value is greater than 0, a positive spatial correlation exists whereas a value lower than 0 indicates a negative spatial clustering pattern. When $I = 0$, there is no spatial correlation exists and LST presents a random spatial distribution. Furthermore, the z-value was employed to test the significance of Moran's I index, which is expressed as follows:

$$Z_I = \frac{I - E(I)}{\sqrt{Var(I)}} \tag{4}$$

where $E(I)$ and $Var(I)$ represent the expectation and standard deviation of global Moran's I index.

B. Spatial Econometric Model

Based on the above selected variables, the ordinary least square (OLS) regression model was constructed. The formula is as follows:

$$Y = \alpha + X\beta + \varepsilon. \tag{5}$$

The OLS may ignore the mutual influence of LST in geographic space. The spatial econometric model, an extension of the OLS model by incorporating the spatial effects, is appropriate to reveal the spatial correlations of variables and produce robust results. The specific model is given by the following formula:

$$\begin{aligned} Y_{it} &= \alpha_i + \rho \sum_{j=1}^{n} W_{ij} Y_{jt} + \beta X_{it} + \theta \sum_{j=1}^{n} W_{ij} X_{jt} + \mu_i \\ \mu_i &= \lambda W \mu_i + \varepsilon_i \end{aligned} \tag{6}$$

where i and j denote different regions and t is sample year. α_i is a vector of intercept. Y_{it} and X_{it} represent LST and its driving factors per district. W_{ij} is the spatial weight matrix. ρ and θ are spatial regression coefficients on the explained variable and independent variable, respectively, implying the spatial interaction between different units. β represents spatial regressive coefficients reflecting the influence of X_{it} on Y_{it}, and λ is the spatial error regression coefficient, reflecting the spatial autocorrelation between error terms. ε_i denotes a vector of regression residuals.

If $\rho \neq 0$, the spatial panel model could calculate total effects, direct effects, and indirect effects through the partial derivatives method [55]. The direct effects are interpreted as the average impact of the independent variable on the interior of the region, whereas the indirect effects (spatial spillover effects) represent the impact of the explanatory variable on the surrounding areas. The total effects are the summation of direct and indirect effects, representing the average impact of the explanatory variable on all units. It can be expressed by the following formula:

$$\frac{\partial Y}{\partial X} = (I_n - \rho W)^{-1} (I_n \beta + W\theta) \tag{7}$$

where $(I_n - \rho W)^{-1}(I_n \beta + W\theta)$ is a $N * N$ matrix, reflecting the impact of the independent variable on the explained variable. It is a function of the spatial weight matrix, thus, can be represented by $S(W)$. The formula (7) can be transformed as follows:

$$\frac{\partial y_i}{\partial x_j} = S(W_{ij}). \tag{8}$$

It is shown that the explanatory variable of region j may be linked to the dependent variable of region i. Typically, when $i = j$, the function indicates the impact of the explanatory variable on its local region, namely direct effects. It can be calculated by the average of the diagonal elements of the matrix. The indirect and total effects are the average of nondiagonal elements and all elements in the matrix, respectively.

When $\rho \neq 0$ and $\theta = 0$, the formula (6) is the spatial lag model (SLM). When $\lambda \neq 0$, $\rho = 0$ and $\theta = 0$, the formula (6) is the spatial error model (SEM). When $\rho \neq 0$, $\theta \neq 0$, and $\lambda = 0$, the formula (6) is the spatial Durbin model (SDM). The SLM measures endogenous interaction among the dependent variables and quantifies the spatial spillover effects on adjacent regions. The SEM is applied when a given region is impacted by neighbors through the error of the independent variables. It is appropriate to analyze spatial dependence in error terms. The SDM, a general form of spatial econometric models, can be transformed into the SLM and SEM with different coefficient settings. Considering both endogenous and exogenous spatial interactions, the SDM not only measures the spatial lag terms of dependent variables, but also the spatially lagged independent variables affecting dependent variables.

IV. Results

A. Spatiotemporal Distribution of LST

Fig. 2 shows the spatial distribution of Beijing's LST from 2014 to 2018. The LST in Beijing presents an obvious downward trend from 2014 to 2017. The average LST in most regions were above 306 K in 2014, whereas the value in most regions dropped below 304 K in 2017. This mitigation is most significant in western and northern areas including Pinggu, Miyun, Huairou, Yanqing, and Mentougou. However, for some districts in the central areas such as Dongcheng and Xicheng, local thermal

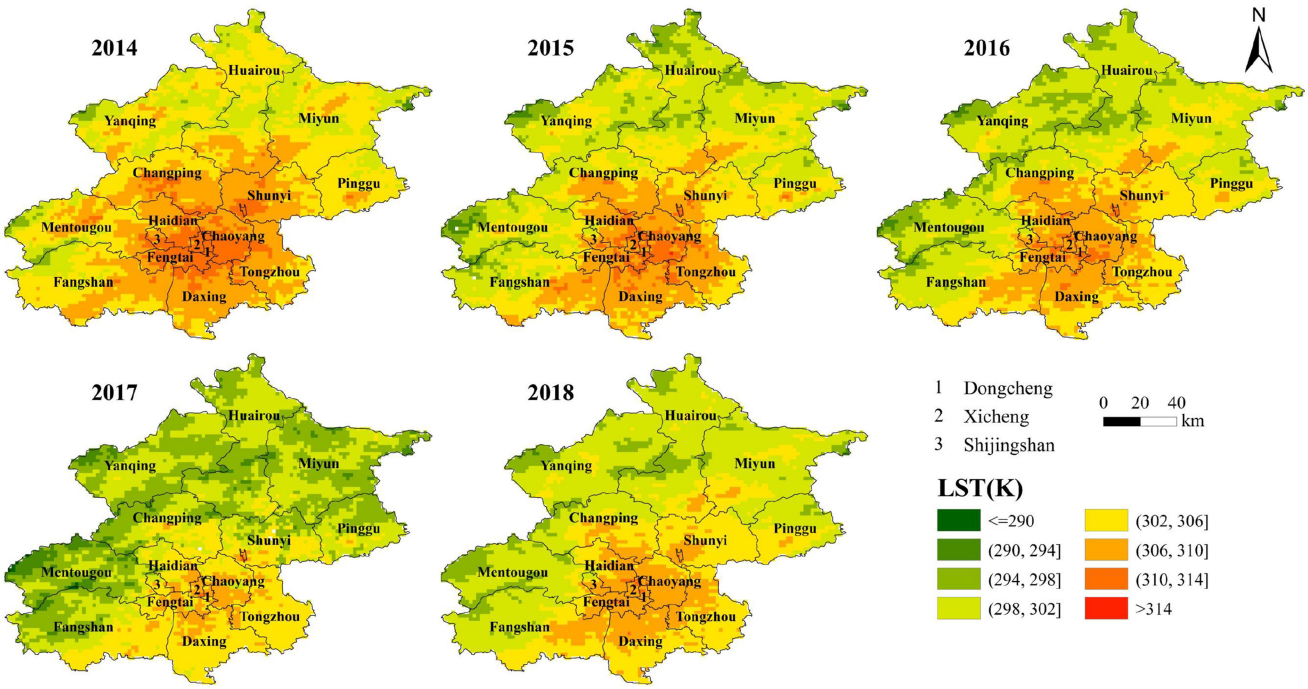

Fig. 2. Spatiotemporal LST patterns from 2014 to 2018.

environments remain severe, though their LST also decreased to some extent. It should be noticed the LST slightly increases in 2018, and the average temperature of each district shows a similar pattern with the value in 2014. Fortunately, the temperature displays a balanced spatial distribution in 2018, with few patches less than 294 K and more than 310 K, compared with that in 2014, indicating several mitigation measures such as energy-saving and emission-reduction have been adopted effectively to relieve urban thermal environments in Beijing.

Under the perspective of spatial, the LST generally presents a low north and high middle distribution pattern. To be more specific, the high temperature areas are mainly concentrated in the middle of Beijing, including Dongcheng, Xicheng, Chaoyang, and Fengtai, with relatively low elevation and large impervious areas. Far from the Beijing central urban area, Miyun, Huairou, and Yanqing have low surface thermal environments where the terrain is high existing with mostly forested land. Among 16 districts in this study, Yanqing always exhibits the lowest annual LST from 2014 to 2018 with a five-year average temperature of 299.6 K. On the contrary, two central districts, Dongcheng and Xicheng, with a five-year average temperature above 309.6 K, are the highest LST areas, although the temperature has decreased from 311 K in 2014.

Furthermore, this article employed global Moran's I index to explore the spatial agglomeration in terms of LST in Beijing from 2014 to 2018, and the results are shown in Table II. Moran's I index displayed a significant decrease in 2016. It is mainly because the Action Plan for Adaptation Strategies for Climate Change in the Urban Area Environment was issued by the Central Government of China, aiming to alleviate urban heat island effects in 2016 [37]. As the capital city of China,

TABLE II
SPATIAL AUTOCORRELATION STATISTICS ON LST

Year	Moran's I	Z-value	P-value
2014	0.509	3.850	0.002
2015	0.532	4.007	0.002
2016	0.479	3.637	0.003
2017	0.549	4.129	0.002
2018	0.506	3.829	0.002

the People's Government of Beijing Municipality designed to construct ventilation corridors to enhance air circulation in the built-up area in the same year [36]. A previous study has also concluded that LST in Beijing decreased in the urban center and increased in the suburban areas [32]. It can be seen that the global Moran's I index, ranging between 0.479 and 0.549, are all greater than 0 and significant at the 1% level (Z-value > 2.58) in five years. These consistently high values illustrate the presence of a significant and positive spatial autocorrelation when investigating urban thermal environments in Beijing at the district level. It means the high urban surface temperature is surrounded by regions with high temperatures and vice versa. Therefore, spatial econometric models are necessary. Besides, the Moran's I in five years changes slightly, indicating Beijing's thermal condition exhibits a stable spatial agglomeration effect.

B. Estimation Results of the Spatial Panel Model

According to the spatial autocorrelation results, Beijing's LST exhibits a significant spatial agglomeration pattern. There is a

TABLE III
RESULTS OF LM, LR, AND WALD TEST

Test	Statistic	P-value
LM spatial lag	19.907***	0.000
LM spatial error	5.204**	0.023
LR (SLM)	36.81***	0.000
LR (SEM)	26.63***	0.001
Wald (SLM)	70.74***	0.000
Wald (SEM)	35.60***	0.000

Note: * $p < 0.1$, ** $p < 0.05$, *** $p < 0.01$

TABLE IV
ESTIMATION RESULTS OF OLS, SLM, SEM, AND SDM

Variable	OLS	SLM	SEM	SDM
ALB	0.123	-0.192	0.007	-0.069
	(0.217)	(0.117)	(0.075)	(0.129)
SLO	-0.061	-0.718**	-0.037	-0.069
	(0.559)	(0.294)	(0.190)	(0.274)
ELE	0.115	0.012	-0.184***	-0.138**
	(0.092)	(0.048)	(0.044)	(0.063)
$NDVI$	0.121***	0.044**	-0.051**	-0.088***
	(0.030)	(0.019)	(0.023)	(0.022)
$MNDWI$	0.260***	0.076*	-0.158***	-0.189***
	(0.073)	(0.045)	(0.058)	(0.056)
NTL	-0.072*	-0.053***	0.011	0.083***
	(0.039)	(0.020)	(0.017)	(0.027)
IA	0.632***	0.368***	0.176**	0.152**
	(0.130)	(0.074)	(0.068)	(0.071)
GDP	-0.148**	-0.076**	0.018	0.003
	(0.065)	(0.034)	(0.272)	(0.026)
PD	0.012	-0.013	0.385**	-0.058
	(0.048)	(0.024)	(0.158)	(0.037)
FEC	0.050	0.039***	-0.008	0.022
	(0.030)	(0.015)	(0.010)	(0.024)
$W*Y$		0.535***		0.606***
		(0.075)		(0.154)
$W*\mu$			0.930***	
			(0.030)	
$W*ALB$				-0.485*
				(0.265)
$W*SLO$				0.853
				(1.064)
$W*ELE$				0.366***
				(0.116)
$W*NDVI$				0.134**
				(0.056)
$W*MNDWI$				0.300***
				(0.093)
$W*NTL$				1.843*
				(0.944)
$W*IA$				0.326
				(0.276)
$W*GDP$				-0.555***
				(0.149)
$W*PD$				-0.542***
				(0.132)
$W*FEC$				0.262**
				(0.115)
$Intercept$	5.686***	2.676***	5.713***	2.285***
	(0.031)	(0.422)	(0.010)	(0.885)
R^2	0.9321	0.9616	0.9885	0.9917

Note: Standard errors in parentheses. (* $p < 0.1$, ** $p < 0.05$, *** $p < 0.01$)

spatial correlation in the explained variable, while the traditional econometric models fail to capture spatial effects. Lagrange multiplier (LM) test is further employed to verify the effects of spatial lag term and spatial error term in an ordinary panel model. As shown in Table III, the null hypothesis of no spatial dependence is rejected because LM spatial lag and LM spatial error are significant at the 1% and 5% levels, respectively. Therefore, the spatial econometric model is introduced to understand the spatial relationship between LST and its drivers. Typically, the spatial models mainly include the SLM, SEM, and SDM.

The regression results of OLS, SLM, SEM, and SDM, using the same independent variables, are compared to understand the relationship between LST and its factors in Beijing (see Table IV). Overall, the goodness-of-fit of spatial econometric models, namely SLM, SEM, and SDM, are 96.16%, 98.85%, and 99.17%, respectively, significantly larger than the R^2 of OLS, indicating the spatial panel models are more appropriate to explain the influence of independent variables on LST. The SDM provides the best fitness to the influential factors, both practically and statistically. In terms of the spatial lag effects, rho ($W*Y$), are similar and significant in the SLM ($\rho = 0.535$, $P = 0.000$) and SDM ($\rho = 0.606$, $P = 0.000$), which means the endogenous interaction relationships exist in the urban thermal environments. Every 1% increase in the LST of surrounding areas will lead to more than 0.5% increase in LST of the local district. The spatial parameter in the SEM, lambda ($W*\mu$), is also statistically significant at the 1% level, which is caused by the spatial effects among interference terms.

We further compare the results of four models. The coefficients of albedo in all models are nonsignificant, and we are likely to conclude that albedo has no relationship with urban thermal condition. However, the spatial spillover coefficient of albedo ($W*\mathrm{ALB}$) in the SDM exhibits a negative effect at the significant level of 10%, suggesting an increase in albedo in adjacent regions would result in the mitigation of LST in local regions. The traditional regression models cannot accurately capture the driving mechanisms of LST. The coefficient of slope in the SLM is negatively significant and the value is much larger than those in other models. The coefficients of elevation, NDVI, and MNDWI display the same characteristics among four models, where the coefficients in the OLS and SLM are positive whereas those in the SEM and SDM are significantly negative. It is widely acknowledged that the temperature decreases as altitude increases. A large body of literatures have concluded that "cold island" such as vegetation and water can mitigate urban thermal environments [51], [56], [57]. In contrast to the coefficient of nighttime light presenting positively significant in the SDM, the coefficient in the OLS and SLM is negative and in the SEM is nonsignificant. Guo *et al.* [14] and Mpakairi and Muvengwi [53] revealed the relationship between nighttime light and LST is positive because nighttime light is positively linked to social economy and urbanization dynamics during the night. The coefficient of impervious area in the SDM presents a positive effect at the significant level. It is smaller than the values in other models, indicating that the influence of impervious areas is overestimated by others. Results of the SDM show that three socio-economic indicators, namely GDP, population

density, and fossil energy consumption, have nonsignificant coefficients with LST. On one hand, the spatial agglomeration of anthropogenic activities and greenhouse gas emissions may cause higher temperatures in urban areas. On the other hand, the concentration of qualified personnel and investment promotes technological innovation in urban, e.g., the elimination of backward production capacity and the development of clean energy, which may decrease the urban temperature.

Some interesting findings are discovered when considering the spatial effects of independent variables based on the SDM. At the 1% level, elevation and MNDWI of surrounding areas have significantly positive spatial effects on the LST, whereas GDP and population density have negative relationships. The spatial correlation coefficients of NDVI and fossil energy consumption are positive and significant at the 5% level. The spatial effect of albedo is negative whereas nighttime light displays a positive effect at the significant level of 10%. And the slope and impervious area of neighbors have nonsignificant effects on LST. As shown in the results, a 1% increase in NDVI and MNDWI of surrounding regions would lead to a 0.134% and 0.3% increase in local regions. The upward land use type in vegetation and water body constrains the expansion of construction buildings, resulting in the reduction of land surface albedo and the mitigation of local thermal condition. It may accelerate the shifting of manufacturing industries to surroundings, which promotes spatial spillover effects and leads to the increase of LST in the industrial receiving areas of adjacent regions. An increase of 1% in GDP and population density of adjacent areas would lead to a 0.555% and 0.542% decrease in local regions. A lot of investment and populations would be attracted with the rapid development of economy and the exploration of population in the adjacent regions. Consequently, local anthropogenic activities may decline due to shortage of funds and departure of the labor force, thereby decreasing the temperature of the land surface. Fossil energy consumption and nighttime light in surrounding areas have positive impacts on LST in local areas, mainly because local areas would also learn from their neighbors as they engage in production and economic activities. This result is consistent with the result of Su and Yu [58], who have concluded that the reduction of energy consumption in an area would cause a decrease in adjacent regions.

C. Direct and Indirect Effects of the Drivers

The SLM and SDM could both estimate spatial effects. However, the spillover effects in the SLM are indistinguishable for every single independent variable, and the SDM always produce more robust result than SLM [59]. Besides, the likelihood ratio (LR) and Wald test are to estimate the SDM whether can be simplified to the SLM or SEM. The null hypotheses of the test are $H_0^{\mathrm{SLM}}: \theta = 0$ and $H_0^{\mathrm{SEM}}: \theta + \rho\beta = 0$. As shown in Table III, the results of LR and Wald test are all significant at the 1% level, which means that the null hypothesis should be rejected and the SDM provides the optimal fitting. Through practical considerations and statistical tests, we estimated the direct, indirect, and total effects of driving factors to interpret the model deeply based on SDM.

TABLE V
DIRECT, INDIRECT, AND TOTAL EFFECTS OF VARIABLES

Variable	Direct effects	Indirect effects	Total effects
ALB	-0.184	-1.344	-1.528
	(0.210)	(1.353)	(1.527)
SLO	0.190	2.821	3.012
	(0.656)	(6.445)	(7.031)
ELE	-0.066	0.732	0.666
	(0.076)	(0.658)	(0.707)
NDVI	-0.071	0.179	0.109
	(0.025)	(0.188)	(0.201)
MNDWI	-0.144	0.470	0.327
	(0.059)	(0.302)	(0.324)
NTL	0.147	0.689	0.836
	(0.065)	(0.659)	(0.716)
IA	0.247	1.053	1.299
	(0.093)	(1.106)	(1.175)
GDP	-0.133	-1.500	-1.633
	(0.091)	(1.149)	(1.236)
PD	-0.204	-1.618	-1.822
	(0.119)	(1.222)	(1.335)
FEC	0.095	0.772	0.867
	(0.072)	(0.830)	(0.896)

Note: Standard errors in parentheses.

The total effects of albedo, GDP, and population density present negative relationships with the agglomeration of LST, whereas the effects of other variables are positively correlated. It is worth noticing that the coefficients on indirect effects (spillover effects) are greater than their direct effects (local effects), showing that urban thermal condition is an interregional issue and adjacent areas mutually affect the temperature to a considerable degree, even greater than the influence on themselves. Similarly, Zhou *et al.* [28] and Feng *et al.* [60] found that the indirect effects of some factors are greater than their direct effects in the study of air pollution. Therefore, joint mitigation measures should be taken based on an overall perspective to solve urban thermal environment issues as a whole (see Table V).

The direct effects of NDVI and MNDWI are negative and the indirect effects are positive. It is mainly because that the increase in woodlands, grasslands, and water bodies relieves the pressure of local heat island effects, which accelerates the expansion of the built-up areas and economic activities in neighboring regions, thereby increasing LST. The local and spillover effects of nighttime light, impervious area, and fossil energy consumption are positive. The effect of impervious area is the largest, followed by that of nighttime light and fossil energy consumption. Nighttime light is widely applied to represent anthropogenic activities such as the construction of built-up areas and the consumption of energy. The aggregation of human activities not only triggers local thermal environments but also LST in adjacent areas. The effects of GDP and population density are significantly negatively correlated with the agglomeration of LST, suggesting they may mitigate the local and adjacent thermal condition of the land surface. The Chinese government has committed to formulating related reports and regulations to ensure the transition

from high-speed growth to high-quality development since the 19th National Congress of the Communist Party of China in 2017. As the capital of China, Beijing undoubtedly becomes the pioneer of economic transition. With flourish in high and new technology industries and modern services, a large crowd of talents thronged, which decreases urban thermal environments effectively and promotes sustainable development.

V. Discussion

A. Driving Factor of LST

City is a complex system comprising mixtures of nature, economy, and society, and changes in urban environments are influenced by many factors [61], [62]. The utilization of multisource data would provide more accurate results [63]. Ten variables under four dimensions included solar radiation, topographical features, surface biophysical parameters, and socio-economic indicators, were selected in this article. Compared with previous studies on LST using grid units, this article employed the existing administrative units, which can avoid choosing the optimal spatial solutions. The selected grid size will affect the relationship between LST and its influencing factors to a certain extent [24], [64], [65]. We explored LST at the district level, which not only facilitates the formulation and implementation of heat island effect mitigation strategies [8], [39], but also enriches our driving factors with data from the statistics department, such as regional fossil energy consumption. Beijing, the capital city of China, is a center of human activities and abundant energy fuels have been consumed [66], [67]. Anthropogenic heat is a prominent factor influencing the local thermal condition [7], so fossil energy consumption should be considered when exploring the driving mechanism of LST effectively.

B. Selection of Spatial Econometric Method

Traditional regression methods are commonly adopted to analyze the impact on LST [17], [68]–[71], ignoring the influence of adjacent areas on thermal environments among regions. As a result, they cannot accurately reflect interregional spatial heterogeneity [72]. Cities are open ecological systems and have mutual effects on each other. Spatial econometric models are identified to capture the spatial aggregation and spillover effects [55]. In this article, the SDM was employed to understand both the direct and indirect spatial effects. It might shed light on the spatial autocorrelation of LST among regions, which is crucial for interregional mitigation measures implications.

C. Limitations

There are some limitations of this article. The primary concern is data acquisition. We only considered the spatial characteristics of LST on an annual basis due to poor data quality (cloud cover), although the temperature displays the dissimilarity between various seasons as well as night and day. Further studies should explore the seasonal, even daily patterns of LST to draw broader conclusions. Additionally, the study investigated the driving mechanisms from a global-space perspective, ignoring the spatial nonstationarity among regions. The present model could be improved with an exploration of local regression model, e.g., geographically weighted regression, further enhancing its accuracy and reliability.

VI. Conclusion

Multisource remote sensing and statistical data from 2014 to 2018 were employed to capture the spatial-temporal characteristics of LST in Beijing at a district level, as well as the analysis of driving mechanisms from the perspective of local and spillover effects based on a spatial econometric model. The main conclusions derived from this article are as follows.

1) The LST of Beijing shows a significant decrease trend from 2014 to 2017, and increases slightly in 2018. Regions with high LST are agglomerated in the central regions, whereas the northern suburban areas have a lower temperature of the land surface. According to the results of Moran's I index, ranging between 0.479 and 0.549, there is a significantly positive spatial autocorrelation of LST in Beijing. Specifically, the districts with high thermal environments are adjacent in geographic space and the low LST regions are also surrounded by each other in space.
2) In contrast to some previous studies, we investigated spatial interactions of independent variables in surrounding areas using the SDM. The results indicate that every 1% increase in LST of adjacent regions would lead to more than 0.6% increase of local regions. With respect to exogenous spatial interactions of independent variables, elevation, NDVI, MNDWI, nighttime light, and fossil energy consumption of neighboring areas show significantly positive spatial effects on local LST, whereas the spatial agglomeration of albedo, GDP, and population density of surroundings display negative effects on LST in local areas.
3) By estimating the spatial effects of influencing drivers based on spatial econometrics, we found that albedo, GDP, and population density are negative factors for LST, whereas other variables exhibit positive correlations with LST. In addition, the coefficients on indirect effects are clearly greater than their direct effects, showing surrounding areas affect the temperature of local regions considerably, even larger than the influence on themselves. Therefore, mutual prevention and control measures should be taken to mitigate thermal environments as a whole, which can strengthen the cooperation among adjacent areas and promote a win–win situation.

References

[1] Y. Wang *et al.*, "Spatial distribution and influencing factors on urban land surface temperature of twelve megacities in China from 2000 to 2017," *Ecological Indicators*, vol. 125, Jun. 2021, Art. no. 107533, doi: 10.1016/j.ecolind.2021.107533.

[2] Y. Rao *et al.*, "Effect of urban growth pattern on land surface temperature in China: A multi-scale landscape analysis of 338 cities," *Land Use Policy*, vol. 103, Apr. 2021, Art. no. 105314, doi: 10.1016/j.landusepol.2021.105314.

[3] United Nations, "Revision of world urbanization prospects," United Nations, New York, NY, USA, 2018. [Online]. Available: https://www.un.org/development/desa/publications/2018-revision-of-world-urbanization-prospects.html

[4] T. Panagopoulos, J. A. González Duque, and M. Bostenaru Dan, "Urban planning with respect to environmental quality and human well-being," *Environ. Pollut.*, vol. 208, pp. 137–144, Jan. 2016, doi: 10.1016/j.envpol.2015.07.038.

[5] M. K. Firozjaei *et al.*, "A new approach for modeling near surface temperature lapse rate based on normalized land surface temperature data," *Remote Sens. Environ.*, vol. 242, Jun. 2020, Art. no. 111746, doi: 10.1016/j.rse.2020.111746.

[6] Y. Chang *et al.*, "Exploring diurnal thermal variations in urban local climate zones with ECOSTRESS land surface temperature data," *Remote Sens. Environ.*, vol. 263, Sep. 2021, Art. no. 112544, doi: 10.1016/j.rse.2021.112544.

[7] X. Li *et al.*, "Urban heat island impacts on building energy consumption: A review of approaches and findings," *Energy*, vol. 174, pp. 407–419, May 2019, doi: 10.1016/j.energy.2019.02.183.

[8] J. Yang *et al.*, "Optimizing local climate zones to mitigate urban heat island effect in human settlements," *J. Cleaner Prod.*, vol. 275, Dec. 2020, Art. no. 123767, doi: 10.1016/j.jclepro.2020.123767.

[9] B. Mashhoodi, D. Stead, and A. van Timmeren, "Land surface temperature and households' energy consumption: Who is affected and where?," *Appl. Geography*, vol. 114, Jan. 2020, Art. no. 102125, doi: 10.1016/j.apgeog.2019.102125.

[10] M. Lemus-Canovas *et al.*, "Estimating barcelona's metropolitan daytime hot and cold poles using landsat-8 land surface temperature," *Sci. Total Environ.*, vol. 699, Jan. 2020, Art. no. 134307, doi: 10.1016/j.scitotenv.2019.134307.

[11] H. You *et al.*, "Spatial evolution of population change in northeast China during 1992–2018," *Sci. Total Environ.*, vol. 776, Jul. 2021, Art. no. 146023, doi: 10.1016/j.scitotenv.2021.146023.

[12] N. R. Mahanta and A. K. Samuel, "Study of land surface temperature (LST) and land cover for urban heat island (UHI) analysis in dubai," in *Proc. 8th Int. Conf. Rel. Infocom Technol. Optim. (Trends Future Directions)*, 2020, pp. 1285–1288, doi: 10.1109/ICRITO48877.2020.9198038.

[13] Z. Xing *et al.*, "Estimation of daily mean land surface temperature at global scale using pairs of daytime and nighttime MODIS instantaneous observations," *ISPRS J. Photogramm. Remote Sens.*, vol. 178, pp. 51–67, Aug. 2021, doi: 10.1016/j.isprsjprs.2021.05.017.

[14] A. Guo *et al.*, "Influences of urban spatial form on urban heat island effects at the community level in China," *Sustain. Cities Soc.*, vol. 53, Feb. 2020, Art. no. 101972, doi: 10.1016/j.scs.2019.101972.

[15] P. Saha *et al.*, "Multi-approach synergic investigation between land surface temperature and land-use land-cover," *J. Earth Syst. Sci.*, vol. 129, Feb. 2020, Art. no. 74, doi: 10.1007/s12040-020-1342-z.

[16] N. R. Govind and H. Ramesh, "The impact of spatiotemporal patterns of land use land cover and land surface temperature on an urban cool island: A case study of Bengaluru," *Environ. Monit. Assess.*, vol. 191, Apr. 2019, Art. no. 283, doi: 10.1007/s10661-019-7440-1.

[17] Y. Liu, J. Peng, and Y. Wang, "Application of partial least squares regression in detecting the important landscape indicators determining urban land surface temperature variation," *Landscape Ecology*, vol. 33, no. 7, pp. 1133–1145, Jul. 2018, doi: 10.1007/s10980-018-0663-7.

[18] L. Gulbe, V. Caune, and G. Korats, "Urban area thermal monitoring: Liepaja case study using satellite and aerial thermal data," *Int. J. Appl. Earth Obs. Geoinformation*, vol. 63, pp. 45–54, Dec. 2017, doi: 10.1016/j.jag.2017.07.005.

[19] C. Bartesaghi-Koc, P. Osmond, and A. Peters, "Mapping and classifying green infrastructure typologies for climate-related studies based on remote sensing data," *Urban Forestry Urban Greening*, vol. 37, pp. 154–167, Feb. 2019, doi: 10.1016/j.ufug.2018.11.008.

[20] A. Sekertekin and E. Zadbagher, "Simulation of future land surface temperature distribution and evaluating surface urban heat island based on impervious surface area," *Ecological Indicators*, vol. 122, Mar. 2021, Art. no. 107230, doi: 10.1016/j.ecolind.2020.107230.

[21] J. Song *et al.*, "Effects of building density on land surface temperature in China: Spatial patterns and determinants," *Landscape Urban Plan*, vol. 198, Jun. 2020, Art. no. 103794, doi: 10.1016/j.landurbplan.2020.103794.

[22] C. Gómez-Navarro *et al.*, "Effects of vegetation on the spatial and temporal variation of microclimate in the urbanized Salt lake valley," *Agricultural Forest Meteorol.*, vol. 296, Jan. 2021, Art. no. 108211, doi: 10.1016/j.agrformet.2020.108211.

[23] I. Grigorescu *et al.*, "Socio-economic and environmental vulnerability to heat-related phenomena in bucharest metropolitan area," *Environ. Res.*, vol. 192, Jan. 2021, Art. no. 110268, doi: 10.1016/j.envres.2020.110268.

[24] J. Yang *et al.*, "Understanding land surface temperature impact factors based on local climate zones," *Sustain. Cities Soc.*, vol. 69, Jun. 2021, Art. no. 102818, doi: 10.1016/j.scs.2021.102818.

[25] P. Vahmani and A. D. Jones, "Water conservation benefits of urban heat mitigation," *Nat. Commun.*, vol. 8, Oct. 2017, Art. no. 1072, doi: 10.1038/s41467-017-01346-1.

[26] J. He *et al.*, "The impact of the terrain effect on land surface temperature variation based on landsat-8 observations in mountainous areas," *Int. J. Remote Sens.*, vol. 40, no. 5/6, pp. 1808–1827, Mar. 2019, doi: 10.1080/01431161.2018.1466082.

[27] H. Liu *et al.*, "The effect of natural and anthropogenic factors on haze pollution in Chinese cities: A spatial econometrics approach," *J. Cleaner Prod.*, vol. 165, pp. 323–333, Nov. 2017, doi: 10.1016/j.jclepro.2017.07.127.

[28] H. Zhou *et al.*, "Directional spatial spillover effects and driving factors of haze pollution in North China plain," *Resour. Conservat. Recycling*, vol. 169, Jun. 2021, Art. no. 105475, doi: 10.1016/j.resconrec.2021.105475.

[29] J. Hu *et al.*, "Analysis of the spatial and temporal variations of land surface temperature based on local climate zones: A case study in Nanjing, China," *IEEE J. Sel. Topics Appl. Earth Observ. Remote Sens.*, vol. 12, no. 11, pp. 4213–4223, Jul. 2019, doi: 10.1109/JSTARS.2019.2926502.

[30] C. Alexander, "Influence of the proportion, height and proximity of vegetation and buildings on urban land surface temperature," *Int. J. Appl. Earth Obs. Geoinformat.*, vol. 95, Mar. 2021, Art. no. 102265, doi: 10.1016/j.jag.2020.102265.

[31] T. Mushore *et al.*, "Predicting urban growth and implication on urban thermal characteristics in Harare, Zimbabwe," in *Proc. IEEE Int. Geosci. Remote Sens. Symp.*, 2018, pp. 846–849, doi: 10.1109/IGARSS.2018.8517625.

[32] X. Liu *et al.*, "Spatiotemporal patterns of summer urban heat island in Beijing, China using an improved land surface temperature," *J. Cleaner Prod.*, vol. 257, Jun. 2020, Art. no. 120529, doi: 10.1016/j.jclepro.2020.120529.

[33] Y. Park, J.-M. Guldmann, and D. Liu, "Impacts of tree and building shades on the urban heat island: Combining remote sensing, 3D digital city and spatial regression approaches," *Comput. Environ. Urban Syst.*, vol. 88, Jul. 2021, Art. no. 101655, doi: 10.1016/j.compenvurbsys.2021.101655.

[34] P. E. Osborne and T. Alvares-Sanches, "Quantifying how landscape composition and configuration affect urban land surface temperatures using machine learning and neutral landscapes," *Comput. Environ. Urban Syst.*, vol. 76, pp. 80–90, Jul. 2019, doi: 10.1016/j.compenvurbsys.2019.04.003.

[35] A. Trlica *et al.*, "Albedo, land cover, and daytime surface temperature variation across an urbanized landscape," *Earth's Future*, vol. 5, no. 11, pp. 1084–1101, Nov. 2017, doi: 10.1002/2017EF000569.

[36] Y. Zhou *et al.*, "Mapping local climate zones and their associated heat risk issues in Beijing: Based on open data," *Sustain. Cities Soc.*, vol. 74, Nov. 2021, Art. no. 103174, doi: 10.1016/j.scs.2021.103174.

[37] Z. Wu, L. Yao, and Y. Ren, "Characterizing the spatial heterogeneity and controlling factors of land surface temperature clusters: A case study in Beijing," *Building Environ.*, vol. 169, Feb. 2020, Art. no. 106598, doi: 10.1016/j.buildenv.2019.106598.

[38] L. Yao *et al.*, "How the landscape features of urban green space impact seasonal land surface temperatures at a city-block-scale: An urban heat island study in Beijing, China," *Urban Forestry Urban Greening*, vol. 52, Jun. 2020, Art. no. 126704, doi: 10.1016/j.ufug.2020.126704.

[39] C. Yin *et al.*, "Effects of urban form on the urban heat island effect based on spatial regression model," *Sci. Total Environ.*, vol. 634, pp. 696–704, Sep. 2018, doi: 10.1016/j.scitotenv.2018.03.350.

[40] L. Hou, W. Yue, and X. Liu, "Spatiotemporal patterns and drivers of summer heat island in Beijing-Tianjin-Hebei urban agglomeration, China," *IEEE J. Sel. Topics Appl. Earth Observ. Remote Sens.*, vol. 14, pp. 7516–7527, Jul. 2021, doi: 10.1109/JSTARS.2021.3094559.

[41] L. Yao *et al.*, "Understanding the spatiotemporal pattern of the urban heat island footprint in the context of urbanization, a case study in Beijing, China," *Appl. Geography*, vol. 133, Aug. 2021, Art. no. 102496, doi: 10.1016/j.apgeog.2021.102496.

[42] S. Liang *et al.*, "The global land surface satellite (GLASS) product suite," *Bull. Amer. Meteorol. Soc.*, vol. 102, no. 2, pp. E323–E337, Feb. 2021, doi: 10.1175/BAMS-D-18-0341.1.

[43] Q. Liu *et al.*, "Preliminary evaluation of the long-term GLASS albedo product," *Int. J. Digit. Earth*, vol. 6, pp. 69–95, Dec. 2013, doi: 10.1080/17538947.2013.804601.

[44] Y. Xiang *et al.*, "Seasonal variations of the dominant factors for spatial heterogeneity and time inconsistency of land surface temperature in an urban agglomeration of central China," *Sustain. Cities Soc.*, vol. 75, Dec. 2021, Art. no. 103285, doi: 10.1016/j.scs.2021.103285.

[45] P. Gong *et al.*, "Annual maps of global artificial impervious area (GAIA) between 1985 and 2018," *Remote Sens. Environ.*, vol. 236, Jan. 2020, Art. no. 111510, doi: 10.1016/j.rse.2019.111510.
[46] J. Peng *et al.*, "Seasonal contrast of the dominant factors for spatial distribution of land surface temperature in urban areas," *Remote Sens. Environ.*, vol. 215, pp. 255–267, Sep. 2018, doi: 10.1016/j.rse.2018.06.010.
[47] C. D. Elvidge *et al.*, "Annual time series of global VIIRS nighttime lights derived from monthly averages: 2012 to 2019," *Remote Sens.*, vol. 13, Mar. 2021, Art. no. 922, doi: 10.3390/rs13050922.
[48] F. Taripanah and A. Ranjbar, "Quantitative analysis of spatial distribution of land surface temperature (LST) in relation ecohydrological, terrain and socio- economic factors based on landsat data in mountainous area," *Adv. Space Res.*, vol. 68, no. 9, pp. 3622–3640, Nov. 2021, doi: 10.1016/j.asr.2021.07.008.
[49] R. Yao *et al.*, "The influence of different data and method on estimating the surface urban heat island intensity," *Ecological Indicators*, vol. 89, pp. 45–55, Jun. 2018, doi: 10.1016/j.ecolind.2018.01.044.
[50] Y. Yu *et al.*, "Interannual spatiotemporal variations of land surface temperature in China from 2003 to 2018," *IEEE J. Sel. Topics Appl. Earth Observ. Remote Sens.*, vol. 14, pp. 1783–1795, Jan. 2021, doi: 10.1109/JSTARS.2020.3048823.
[51] N. Bakr and O. R. Abd El-kawy, "Modeling the artificial lake-surface area change in arid agro-ecosystem: A case study in the newly reclaimed area, Egypt," *J. Environ. Manage.*, vol. 271, Oct. 2020, Art. no. 110950, doi: 10.1016/j.jenvman.2020.110950.
[52] M. Carpio *et al.*, "Influence of pavements on the urban heat island phenomenon: A scientific evolution analysis," *Energy Build*, vol. 226, Nov. 2020, Art. no. 110379, doi: 10.1016/j.enbuild.2020.110379.
[53] K. S. Mpakairi and J. Muvengwi, "Night-time lights and their influence on summer night land surface temperature in two urban cities of Zimbabwe: A geospatial perspective," *Urban Clim.*, vol. 29, Sep. 2019, Art. no. 100468, doi: 10.1016/j.uclim.2019.100468.
[54] Y. B. Attahiru *et al.*, "A review on green economy and development of green roads and highways using carbon neutral materials," *Renewable Sustain. Energ. Rev.*, vol. 101, pp. 600–613, Mar. 2019, doi: 10.1016/j.rser.2018.11.036.
[55] J. P. LeSage and R. K. Pace, *Spatial Econometric Models*. Berlin, Germany: Springer, 2010.
[56] J. Yang *et al.*, "The impact of spatial form of urban architecture on the urban thermal environment: A case study of the Zhongshan district, Dalian, China," *IEEE J. Sel. Topics Appl. Earth Observ. Remote Sens.*, vol. 11, no. 8, pp. 2709–2716, Mar. 2018, doi: 10.1109/JSTARS.2018.2808469.
[57] F. Cui *et al.*, "Quantifying the response of surface urban heat island to urban greening in global north megacities," *Sci. Total Environ.*, vol. 801, Dec. 2021, Art. no. 149553, doi: 10.1016/j.scitotenv.2021.149553.
[58] Y. Su and Y. Yu, "Spatial agglomeration of new energy industries on the performance of regional pollution control through spatial econometric analysis," *Sci. Total Environ.*, vol. 704, Feb. 2020, Art. no. 135261, doi: 10.1016/j.scitotenv.2019.135261.
[59] R. Mínguez, J.-M. Montero, and G. Fernández-Avilés, "Measuring the impact of pollution on property prices in Madrid: Objective versus subjective pollution indicators in spatial models," *J. Geographical Syst.*, vol. 15, no. 2, pp. 169–191, Apr. 2013, doi: 10.1007/s10109-012-0168-x.
[60] T. Feng *et al.*, "Spatial spillover effects of environmental regulations on air pollution: Evidence from urban agglomerations in China," *J. Environ. Manage.*, vol. 272, Oct. 2020, Art. no. 110998, doi: 10.1016/j.jenvman.2020.110998.
[61] J. L. F. Li *et al.*, "Linking global land surface temperature projections to radiative effects of hydrometeors under a global warming scenario," *Environ. Res. Lett.*, vol. 16, Aug. 2021, Art. no. 084044, doi: 10.1088/1748-9326/ac153c.
[62] K. Deilami, M. Kamruzzaman, and Y. Liu, "Urban heat island effect: A systematic review of spatio-temporal factors, data, methods, and mitigation measures," *Int. J. Appl. Earth Obs. Geoinformat.*, vol. 67, pp. 30–42, May 2018, doi: 10.1016/j.jag.2017.12.009.
[63] M. Sahana, S. Dutta, and H. Sajjad, "Assessing land transformation and its relation with land surface temperature in Mumbai city, India using geospatial techniques," *Int. J. Urban Sci.*, vol. 23, no. 2, pp. 205–225, Apr. 2019, doi: 10.1080/12265934.2018.1488604.
[64] S. Anoop *et al.*, "Validation and comparison of LPRM retrieved soil moisture using AMSR2 brightness temperature at two spatial resolutions in the Indian region," *IEEE Geosci. Remote. Sens. Lett.*, vol. 14, no. 9, pp. 1561–1564, Sep. 2017, doi: 10.1109/LGRS.2017.2722542.
[65] P. D. Jones *et al.*, "Adjusting for sampling density in grid box land and ocean surface temperature time series," *J. Geophys. Res.-Atmos.*, vol. 106, no. D4, pp. 3371–3380, Feb. 2001, doi: 10.1029/2000JD900564.
[66] K. Dong *et al.*, "Spatial econometric analysis of China's PM10 pollution and its influential factors: Evidence from the provincial level," *Ecological Indicators*, vol. 96, pp. 317–328, Jan. 2019, doi: 10.1016/j.ecolind.2018.09.014.
[67] B. Wang *et al.*, "Unveiling the driving factors of carbon emissions from industrial resource allocation in China: A spatial econometric perspective," *Energy Policy*, vol. 158, Nov. 2021, Art. no. 112557, doi: 10.1016/j.enpol.2021.112557.
[68] L. Gao *et al.*, "Localization or globalization? determination of the optimal regression window for disaggregation of land surface temperature," *IEEE Trans. Geosci. Remote Sens.*, vol. 55, no. 1, pp. 477–490, Jan. 2017, doi: 10.1109/TGRS.2016.2608987.
[69] P. Fu and Q. Weng, "Variability in annual temperature cycle in the urban areas of the United States as revealed by MODIS imagery," *J. Photogramm. Remote Sens.*, vol. 146, pp. 65–73, Dec. 2018, doi: https://doi.org/10.1016/j.isprsjprs.2018.09.003.
[70] M. E. Hereher, "Retrieving spatial variations of land surface temperatures from satellite data–Cairo region, Egypt," *Geocarto Int.*, vol. 32, no. 5, pp. 556–568, May 2017, doi: 10.1080/10106049.2016.1161077.
[71] M. Zorigt *et al.*, "Modeling permafrost distribution over the river basins of Mongolia using remote sensing and analytical approaches," *Environ. Earth Sci.*, vol. 79, Jun. 2020, Art. no. 308, doi: 10.1007/s12665-020-09055-7.
[72] Y. Wang *et al.*, "Exploring the spatial effect of urbanization on multi-sectoral CO2 emissions in China," *Atmos. Pollut. Res.*, vol. 10, no. 5, pp. 1610–1620, Sep. 2019, doi: 10.1016/j.apr.2019.06.001.

Menghang Liu received the B.S. degree in land resource management from Chang'an University, Xi'an, China, in 2018 and the M.S. degree in natural resources from Beijing Normal University, Beijing, China, in 2021.

His research interests include urban development, regional planning, and big data application.

Haitao Ma received the B.S. degree in geographic science from Ludong University, Yantai, China, in 2004, the M.S. degree in human geography from Henan University, Kaifeng, China, in 2007, and the Ph.D. degree in urban geography from Sun Yat-sen University, Guangzhou, China, in 2010.

Since 2014, he has been an Associate Professor with the Institute of Geographic Sciences and Natural Resources Research, Chinese Academy of Sciences. From 2019 to 2020, he was a Visiting Scholar with Geography Department, University of Utah, Salt Lake City, UT, USA. His current research interest includes urbanization and regional sustainable development.

Yu Bai received the B.S. degree in geographical information science from Shaanxi Normal University, Xi'an, China, in 2018 and the M.S. degree in cartography and geography information system from Beijing Normal University, Beijing, China, in 2021. She is currently working toward the Ph.D. degree in ecology with the University of Chinese Academy of Sciences, Beijing, China.

Her research interests include global change ecology, and applications of remote sensing data for ecosystem.